ENPH 257 Lab Report

Brunette, Jacob   Fullerton, Dilyn   Watt, Ryan   Yao, Dickson

Instructor: Dr. Christopher Waltham

June 30, 2016

Abstract

We attempt to estimate several intrinsic thermal properties of a brass rod by measuring temperature data during heating and cooling and comparing with a simplified one-dimensional model, which attempts to account for the effects of conduction, convection, and radiation. We test the rod under various conditions to observe and characterize the effects of orientation, surface quality, and power input on the heating behavior and thermal qualities of the rod. Thermal parameters are optimized based on the simulation using a Levenberg-Marquardt algorithm. However, the obtained results carry uncertainty values that are too great to be conclusive.

Contents

Chapter 1

Introduction

The purpose of this experiment is to find the parameters that determine heat transport mechanisms along a brass rod; these heat transport mechanisms are thermal conduction, convection and radiation.

1.1 Conduction

Heat diffusion due to conduction is given by the heat equation

$$\left(\frac{\partial}{\partial t}u(\mathbf{r},t)\right)_{\text{cond}} = \frac{k}{c\rho}\nabla^2 u(\mathbf{r},t), \tag{1.1}$$

where $u(\mathbf{r},t)$ is the temperature at position $\mathbf{r}$ and time t, k is the thermal conductivity, c is the specific heat of the material, and ρ is the mass density of the material.

1.2 Convection

Power gain due to convection for a differential surface element at position $\mathbf{r}$ may be approximated by

$$P_{\text{conv}}(\mathbf{r},t) = -k_c\,\delta S(\mathbf{r})\left(u(\mathbf{r},t) - u_{\text{amb}}\right), \tag{1.2}$$

where k_c is the convection coefficient, $\delta S(\mathbf{r})$ is the differential surface element at $\mathbf{r}$, and u_{amb} is the ambient temperature of the surrounding fluid.

Now temperature change due to power for a differential mass element is given by

$$P = \frac{\partial}{\partial t}Q = c\rho\,\delta V\frac{\partial}{\partial t}u, \tag{1.3}$$

so the rate of change of temperature due to convection is given by

$$\left(\frac{\partial}{\partial t}u(\mathbf{r},t)\right)_{\text{conv}} = -\frac{k_c\,\delta S(\mathbf{r})}{c\rho\,\delta V(\mathbf{r})}\left(u(\mathbf{r},t) - u_{\text{amb}}\right). \tag{1.4}$$

1.3 Radiation

Power gain due to radiation for a differential surface element at position $\mathbf{r}$ is given by Planck's Law to be

$$P_{\text{rad}}(\mathbf{r},t) = -\epsilon\,\sigma\,\delta S(\mathbf{r})\left(u(\mathbf{r},t)^4 - u_{\text{amb}}^4\right), \tag{1.5}$$

where ϵ is the emissivity and σ is the Stefan-Boltzmann constant.

Again from Equation (1.3), we can obtain the contribution to the rate of change of temperature due to radiation

$$\left(\frac{\partial}{\partial t}u(\mathbf{r},t)\right)_{\text{rad}} = -\frac{\epsilon\,\sigma\,\delta S(\mathbf{r})}{c\rho\,\delta V(\mathbf{r})}\left(u(\mathbf{r},t)^4 - u_{\text{amb}}^4\right). \tag{1.6}$$

1.4 Heat diffusion equation for a cylindrical rod

For a one-dimensional cylindrical rod of length L and radius R, the heat diffusion equation is

$$\frac{\partial}{\partial t}u(x,t) = \frac{1}{c\rho}\left(k\frac{\partial^2}{\partial x^2}u(x,t) - k_c\frac{\delta S(x)}{\delta V(x)}\left(u(x,t) - u_{\mathrm{amb}}\right) - \epsilon\,\sigma\frac{\delta S(x)}{\delta V(x)}\left(u(x,t)^4 - u_{\mathrm{amb}}^4\right) + \frac{P_{\mathrm{in}}(x,t)}{\delta V(x)}\right), \quad (1.7)$$

where P_{in} is the power input function.

Chapter 2

Method

2.1 Experimental setup

While parts of the apparatus were changed to vary the effects of heat transfer parameters, the rod remained largely unchanged throughout the experiment. However, it was necessary to prepare the brass rod for temperature measurements. A 15 Ω power resistor was screwed onto the end of the rod to provide heat. Thermal paste was dabbed onto the side of the resistor that was fastened against the rod for more efficient thermal conduction. Additionally, four holes aligned on the perimeter of the rod were drilled into one-third of the rod's diameter, where thermocouple sensors were inserted to sample the temperature at each hole. The 3 mm holes were evenly spaced 7.25 cm apart, and the hole nearest to the free end was 1.55 cm from the end of the 33 cm rod. Additionally, the diameter of the rod was measured to be 2.22 cm wide. The thermocouples were then numbered in ascending order from the hole closest to the resistor.
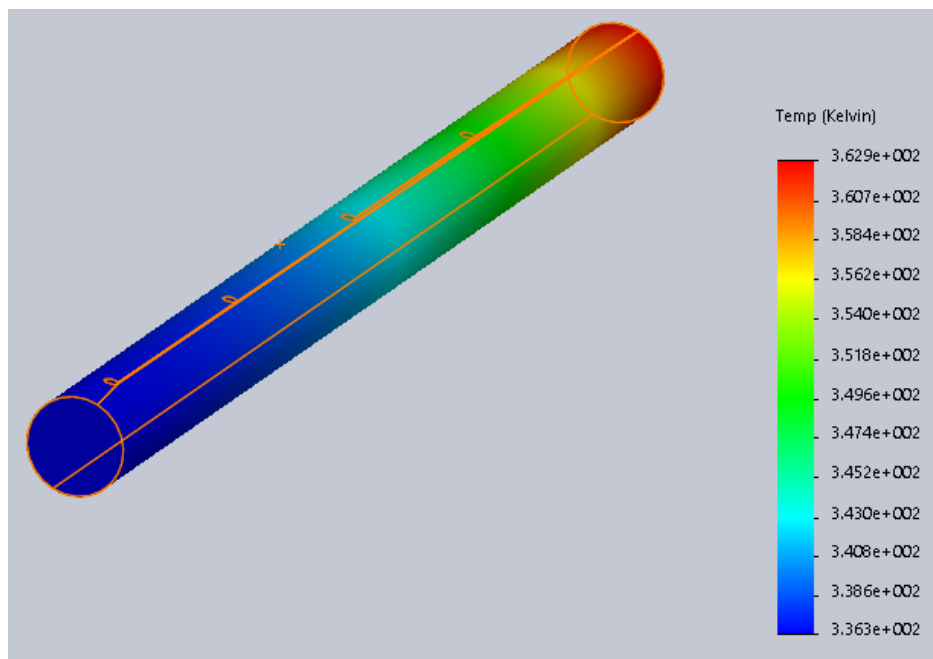

Figure 2.1: Brass rod CAD design

The thermocouples are supported by a circuit (see Figure 2.2) that amplifies their signal, which is then read by an Arduino and processed for a corresponding temperature in MATLAB. Since thermocouples output a minute voltage, on the scale of millivolts, an instrumental amplifier is used to amplify the signal. Following

amplification, the output is connected to an inverter to meet the specifications for the Arduino's analog input, which requires a positive voltage.

The thermocouples are directly connected to the two inputs of a differential amplifier, with a 10 kΩ resistor to ground as is suggested by the manufacturer, with a gain of ~ 1500 to boost their signal to the scale of several volts, which can be read by an Arduino. The signal is then fed through a unity gain inverting operational amplifier so that the signal is primarily in the positive voltage range. At the output of this amplifier, there is a low pass filter consisting of a 220 nF capacitor and a 1 kΩ resistor to ground. The Arduino reads data directly from this filter.
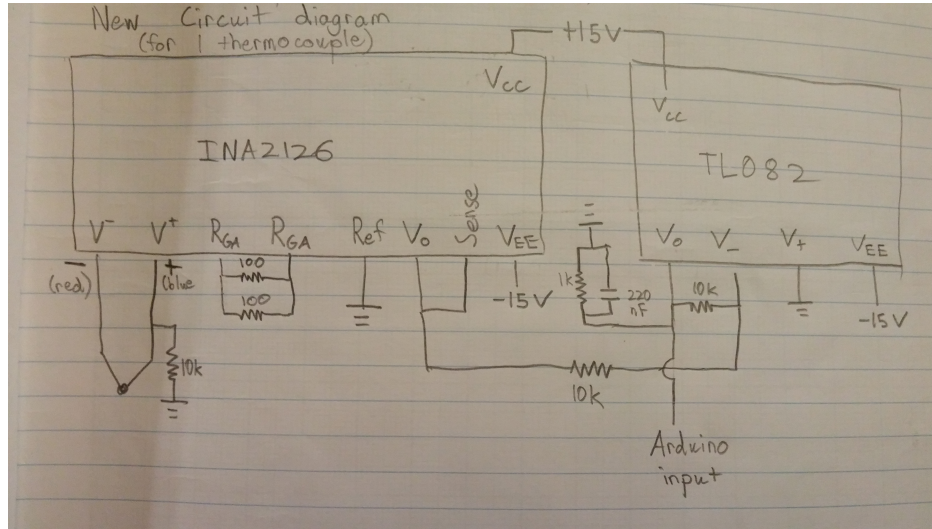

Figure 2.2: Thermocouple circuit diagram

2.2 Calibration

To find a temperature that corresponds to an analog voltage reading, a calibration curve was made for each thermocouple. The thermocouples were placed in a water bath along with a digital thermometer, and the temperature of the bath was varied beginning from a hot-water bath at 70°C, down to around 30°C as cold water was added. The temperature on the digital thermometer was manually inputted into a MATLAB program that recorded the temperature and the voltage that it matched on each thermocouple. Due to the noisy signal from the thermocouple voltage, approximately 10 voltage values were recorded for an individual thermocouple at that temperature, and averaged. Plotting the temperature-voltage plot over several temperatures ranging from 30° to 70°C gives a calibration curve, such as in Figure 2.3. Since an approximately linear relationship is observed, a linear equation converting voltage to temperature was found for each thermocouple using linear regression.

2.3 Data aquisition

Experiments started with collecting the data that determined the heat transfer coefficients as controlled variables. For the control group, the rod was set up hanging vertically, clamped at the end closest to the power resistor. To prevent heat loss by conduction to the clamps, four rubber O-ring bands were wrapped around the rod as an insulating buffer between the rod and clamp. A rough estimate of the desired heating time (to avoid temperatures over 70°C) was found using a high-level simulation. Data collection trials typically ran for one hour, which included data collection while the rod was both heating and cooling.
Next, the experimental setup was changed to alter the heat transfer coefficients. However, multiple experimental trials were run using one particular setup with several different voltage inputs to the power resistor
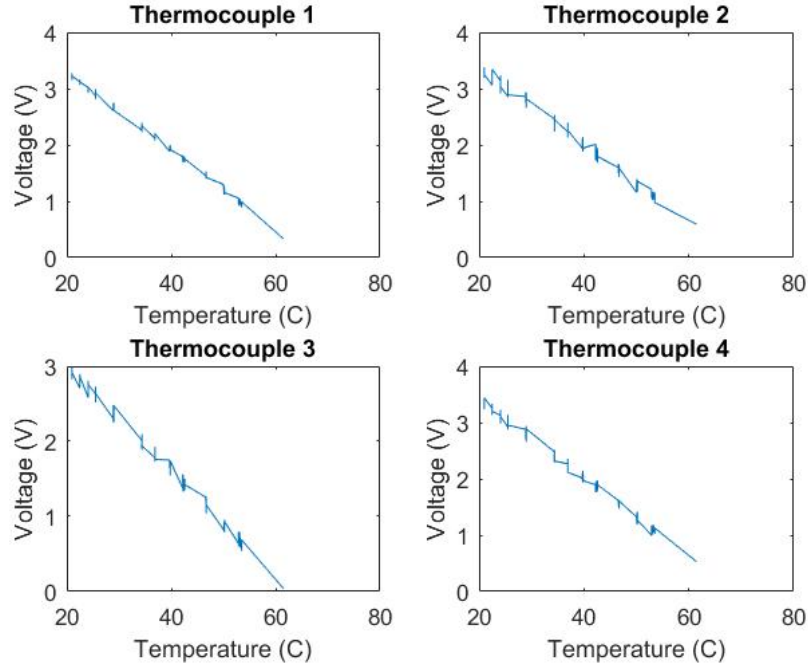
Figure 2.3: Example calibration curves

for repeated data sets. To vary the convective coefficient, the rod was placed in three different positions: horizontally, vertically, and diagonally. In its horizontal position, the rod was held up by two edges of a container and tied down with string to restrict its motion. A stand and ring clamp was used to hold the rod diagonally, where O-rings were used again to minimize heat loss by conduction between the rod and clamp. Then, emissivity was increased by applying black electrical tape over the entire surface of the rod. Finally, the rod was buffed using sandpaper, giving it a polished finish to increase its reflectance. The experiments with varied emissivity had measurements taken in a vertically clamped position.

Chapter 3

Simulation and optimization

3.1 One-dimensional explicit-step simulation

The following is the finite difference equation to simulate heat diffusion based on Equation (1.7) for a cylindrical rod of length L and radius R. Based on the formalism in Appendix A and supposing x points $\{x_i : i \in [0, X]\}$ and t points $\{t_n : n \in [0, T]\}$, the explicit finite difference form of Equation (1.7) is

$$\mathbf{u}^{n+1} = \mathbf{u}^n + \delta t \left(\delta \mathbf{u}^n_{\text{cond}} + \delta \mathbf{u}^n_{\text{conv}} + \delta \mathbf{u}^n_{\text{rad}} + \delta \mathbf{u}^n_{\text{pow}} \right), \tag{3.1}$$

where

$$(\delta \mathbf{u}^n_{\text{cond}})_i = \frac{k}{c\rho} \cdot \frac{1}{\delta x^2} \cdot \begin{cases} u^n_1 - u^n_0, & i = 0 \\ u^n_{X-1} - u^n_X, & i = X \\ u^n_{i-1} - 2u^n_i + u^n_{i+1}, & \text{else} \end{cases}$$

$$(\delta \mathbf{u}^n_{\text{conv}})_i = -\frac{k_c}{c\rho} \cdot \frac{\delta S_i}{\delta V_i} (u^n_i - u_{\text{amb}})$$

$$(\delta \mathbf{u}^n_{\text{rad}})_i = -\frac{\epsilon \sigma}{c\rho} \cdot \frac{\delta S_i}{\delta V_i} \left((u^n_i)^4 - u^4_{\text{amb}} \right)$$

$$(\delta \mathbf{u}^n_{\text{pow}})_i = \frac{P^n_i}{c\rho \, \delta V_i}$$

The differential volume at any point x_i is the same

$$\delta V_i = \pi R^2 \, \delta x.$$

The exposed surface is different at the ends, however, with

$$\delta S_i = 2\pi R \, \delta x + \begin{cases} \pi R^2, & i = 0 \text{ or } i = X \\ 0, & \text{else} \end{cases}$$

Finally power input occurs only at one end. It is assumed that power is a constant P_1 during heating and P_2 during cooling. Heating occurs until t_{stop} at which point cooling begins. Thus we have

$$P^n_i = \begin{cases} P_1, & t_0 < t_n < t_{\text{stop}} \\ P_2, & t_{\text{stop}} \le t_n \le t_T \end{cases}$$

3.2 Optimization of one-dimensional simulation

A numerical optimization routine based on the Levenberg-Marquardt algorithm was used to optimize thermodynamical parameters by repeatedly varying these parameters, running the one-dimensional simulation,

and comparing the results to experimental data until optimal parameters were achieved. This optimization was run for each dataset. Only the data of the two middle thermocouples was used in the optimization, as these were generally much better behaved than the edges. For each optimization, 67 positional points and a time step of .5 seconds were used. The code used is available at `https://github.com/EmceeEscher/Robot-thermo-group`.

3.3   High-level simulation

The heat transfer coefficients that were found through the optimization program were subsequently inputted to produce a high-level simulation of the heating of the rod in ANSYS (see Figure 3.2). Because additional parameters such as initial temperature and density were fitted in the optimization software, a custom material was made possessing these qualities, and initial conditions were set to match the parameters.

The results of the high-level simulation are comparable to the experimental data gathered on June 6th, which used 15.18 V to the power resistor and 15.36 W of heating power, and was set up vertically, prior to being polished. For thermocouples 2 to 4, the temperatures after a 1200 second heating period have approximately a 3°C difference to the simulation. This demonstrates that the parameters derived from the fitting optimization produced plausible (although not completely accurate) values.
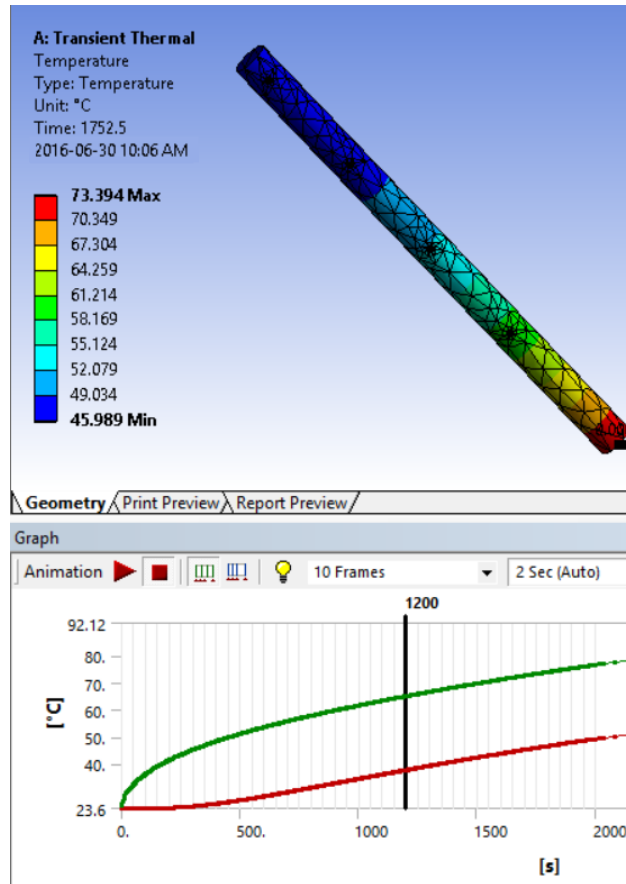
Figure 3.1: Initial ANSYS simulation 7.5 V
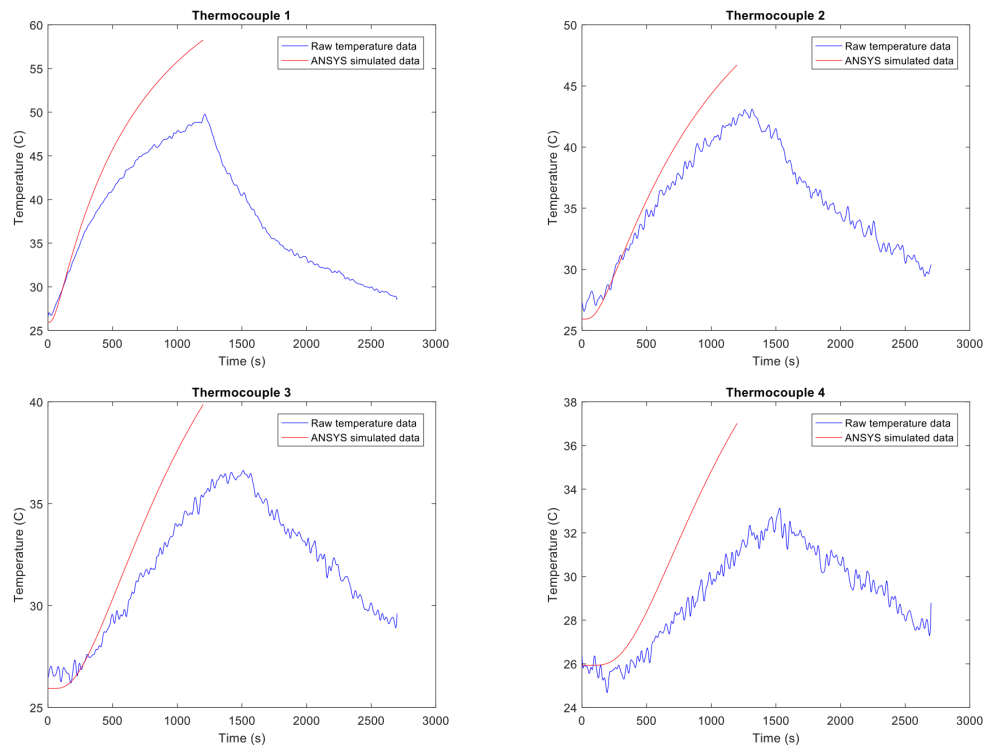
Figure 3.2: Example ANSYS simulation results for thermocouples 1-4

Chapter 4

Results

Results of parameter optimizations are documented in Table 4.2.

Table 4.1: Runs: Descriptions

Run	Potential (V)	Run type	Orientation
May 30 - Run 1	20.30	normal	vertical
May 30 - Run 2	17.70	normal	vertical
June 01 - Run 1	15.18	normal	horizontal
June 03 - Run 1	10.60	normal	diagonal
June 03 - Run 2	15.18	normal	diagonal
June 06 - Run 1	15.18	normal	vertical
June 06 - Run 2	15.18	taped	vertical
June 06 - Run 3	20.30	taped	vertical
June 08 - Run 1	15.18	buffed	vertical
June 08 - Run 3	20.30	buffed	vertical
June 13 - Run 1	15.18	buffed	horizontal

Table 4.2: Runs: Optimization results

Run	k_c	ϵ	ρ	P_1	P_2	c	k	u_0	u_{amb}	Power	Power frac
Vertical											
May 30 - Run 1	12.5668	1	8782.77	25.0745	-1.9987	382.1010	100.0	295.8740	304.3108	27.47267	0.9127
May 30 - Run 2	8.1040	1	8293.50	20.8860	0.0707	361.0000	100.0	301.8020	298.6727	20.88600	1.0000
June 06 - Run 1	8.4069	1	8493.26	13.9178	0.9902	369.6951	100.0	297.6903	297.1670	15.36216	0.9060
June 06 - Run 2	19.1927	0	8370.07	15.3622	3.3211	364.3329	100.0	300.8075	294.2197	15.36216	1.0000
June 06 - Run 3	15.5571	1	8447.59	26.6469	2.5599	367.7051	100.0	300.8720	296.5346	27.47267	0.9699
June 08 - Run 1	4.7554	1	8293.50	12.9929	-0.0267	361.0000	102.9	298.7773	296.1117	15.36216	0.8458
June 08 - Run 3	6.9179	1	8452.08	21.8658	-0.5948	367.8965	100.0	300.3236	301.7212	27.47267	0.7959
Mean	10.7858										
Std Dev	5.1767										
Horizontal											
June 01 - Run 1	05.9338	1	8603.09	13.1600	-0.9993	370.2600	100.0	296.9922	301.6543	15.36216	0.8567
June 13 - Run 1	08.7668	1	8718.01	15.3622	-0.0000	379.9838	100.0	298.1978	300.2710	15.36216	1.0000
Mean	7.3503										
Std Dev	2.0032										
Diagonal											
June 03 - Run 1	05.8893	1	8729.63	07.4374	-0.0149	380.0648	100.0	297.2276	297.7102	07.49067	0.9929
June 03 - Run 2	07.3700	1	8537.28	15.2304	-0.1991	371.9972	100.0	299.6723	299.9362	15.36216	0.9914
Mean	6.6296										
Std Dev	1.0470										
TOTALS											
Mean		0.9091	8520.07			370.5488	100.3	298.9306	298.9372		0.9338
Std Dev		0.3015	171.77			7.4300	0.9	1.9007	2.9581		0.0743

Chapter 5

Analysis

5.1 Quality of optimization

Individual fits

Table 5.1 describes the quality of the individual fits to data from which individual thermodynamical parameters were derived. The slope and intercept are those of the linear regression and should theoretically be 1 and 0 respectively. The R^2 is the square of the correlation coefficient between the simulation and experimental data; a value close to 1 indicates a strong fit. Finally standard error is the standard error of the estimates of slope and intercept.

Table 5.1: Optimization quality: Individual fits

Run	Slope	Intercept	R-squared	Std Err
May 30 - Run 1	0.9998	0.0558	0.9956	0.0010
May 30 - Run 2	1.0635	-19.7122	0.9193	0.0041
June 01 - Run 1	0.9999	0.0251	0.9964	0.0009
June 03 - Run 1	1.0000	0.0110	0.9969	0.0005
June 03 - Run 2	0.9999	0.0298	0.9973	0.0005
June 06 - Run 1	0.9999	0.0257	0.9942	0.0010
June 06 - Run 2	1.0056	-1.7206	0.9912	0.0010
June 06 - Run 3	0.9997	0.1019	0.9826	0.0014
June 08 - Run 1	0.9999	0.0205	0.9986	0.0005
June 08 - Run 3	0.9998	0.0594	0.9971	0.0006
June 13 - Run 1	1.0028	-0.8647	0.9966	0.0006

Average fits

Based on the average values determined in Table 4.2, simulations were run for each trial where the global average values were used for ϵ, ρ, c, and k. Average values for the particular geometry were used for k_c. And specific values were usedfor P_1, P_2, u_0, and u_{amb}, as these are heavily dependent on the particulars of the trial.

Table 5.2: Optimization quality: Average fits

Run	Slope	Intercept	R-squared	Std Err
May 30 - Run 1	0.1915	246.1704	0.4222	0.0034
May 30 - Run 2	0.3282	202.8493	0.7470	0.0025
June 01 - Run 1	0.2619	223.4058	0.4569	0.0043
June 03 - Run 1	0.3522	192.5934	0.7374	0.0019
June 03 - Run 2	0.2800	217.0452	0.6371	0.0022
June 06 - Run 1	0.3420	195.1229	0.6018	0.0035
June 06 - Run 2	0.2935	209.0217	0.8326	0.0014
June 06 - Run 3	0.2691	216.8487	0.8205	0.0013
June 08 - Run 1	0.4113	174.5721	0.6152	0.0042
June 08 - Run 3	0.2540	229.4468	0.4798	0.0028
June 13 - Run 1	0.2650	221.1282	0.5807	0.0023

5.2 Explanation of results

Convective heat transfer coefficient

Our values for the convective heat transfer coefficient had a large range of values (up to 77.5% of the average); thus it is almost meaningless beyond finding the correct order of magnitude of the actual result. A large part of the difficulty in determining k_c is that it is affected by many different variables beyond just geometry, and treating it as a constant is a major approximation. We did not sufficiently isolate the geometry as the only variable affecting k_c, so we were not able to determine its actual value to any degree of certainty.

Emissivity

Although in accordance with Table (4.2) our average value is at 0.91, this does not reflect the actual value of the rod. This is due to the optimization consistently hitting its upper bound of 1.0 and on one occasion reaching its lower bound of 0. These occurrences did not line up with the application of taping or buffing the rod and so we consider our values to be inherently flawed.

Density

The simulation's derived density has no physical relevance as we measured it to be 7971 kg/m^3. Additionally, the simulation had no way to directly calculate the density as it only ever appeared multiplied by the specific heat. In hindsight, the value of density should have been measured early on so as to input the measured value for density instead of letting the program try to fit it.

Power2

This value represents the power loss from the resistor when the rod was cooling. The resistor significantly changed the properties of the end of the rod it was connected to, and we attempted to account for its effect by allowing it to having a negative power input during the cooling period, independent of the heating power. This allowed strong fitting of the full heating/cooling period; however the program sometimes fit an exceedingly large value (or even a positive value) to this power draw, indicating that this model is not likely physically accurate.

Specific heat

The value for specific heat averages to 370 J/g*K, which is a reasonable value with low relative error. A potential issue comes from the fact that its simulation value occasionally reached the imposed lower bound of 361; however, this did not occur frequently enough to shift our bounds on its actual value too far from this average. Therefore, we consider this value to have an uncertainty of 20 J/g*K.

Thermal Conductivity

This value was seen to consistently hit its imposed lower bound of 100 W/m*K in the optimization which tells us most likely that its proper value is well below 100, although no specific numerical approximation can be made with this data.

u_0 and u_{amb}

Instead of manually inputting the starting temperature of the rod and the room, we let the program attempt to optimize for temperatures that led to the best fit of the data. The program generally did a good job of optimizing for a starting temperature and an ambient temperature that were physically reasonable, but it was an unnecessary exercise, and it would have been a better idea to measure these values and input them into the simulation manually, instead of forcing the program try to optimize them.

Power Fraction

The average value of power fraction was found to be 93% which is a reasonable value in this scenario. The simulation frequently placed values under its imposed maximum bound of 100% for this value, and so we assign it an uncertainty of 10%.

5.3   Uncertainty

Lab setup

Thermocouple fluctuations (key source)

Thermocouple readings fluctuated a lot, despite the fact that we fed them into both an instrument amplifier and an op-amp inverter circuit before we tried to do any kind of filtering. Our filtering was effectively a simple low-pass filter which, in practice, did very little. Consequently, consecutive readings of temperatures (converted from the thermocouple voltage readings) had large uncertainties, as they regularly fluctuated with a range of $\pm2°$C for readings taken half a second apart. We tried to smooth out the noise in our data with MATLAB's smoothing functionality, but even the smoothed data had frequent spikes. This had a large effect on all of our future efforts at fitting parameters to the data.

Heat loss of power resistor

The end of the rod with the power resistor had different physical conditions (especially emissivity) than the rest of the rod. Obviously, it was a heat source when plugged in, but it became a heat sink when we unplugged it and allowed the rod to cool. During cooling, the end of the rod closest to the resistor often dropped to lower temperatures than the rest of the rod, most likely due to the presence of the resistor. We attempted to model this in our simulation, using a `power2` parameter to represent of the power lost through the resistor while the rod was cooling. This added another parameter that we needed to fit, however, and possibly made the finite difference model we used into a poorer representation of the physical state of the rod.

Lack of multiple trials:

Due to time constraints, we were unable to run multiple trials for most of our data collection setups, which increased the uncertainty in our data and hampered our ability to catch and correct experimental mistakes. This was especially detrimental to the convective heat transfer coefficient result, which depends the most upon particular experimental setups.

Simulation and optimization

Errors in simulation

The simulation is subjected to certain errors based on the approximations of the finite differencing scheme (see Appendix A). Error in position (Equation (A.9)) is quadratic, and since the simulations used $\delta x = 0.005$ m, the error in the spatial derivative is on the order of 10^{-5} m and thus largely negligible. Error in time (Equation (A.7)) is linear, and since the simulations used $\delta t = 0.25$ s, the error in the time derivative is on the order of 0.1. While the condition for numerical stability (Equation (A.5)) is satisfied, this certainly could have contributed to the error in the final optimized parameter, especially since only a rudimentary explicit scheme was used. Perhaps it would have been useful to implement an implicit scheme, which is guaranteed to be numerically stable, or a a Crank-Nicolson scheme, which is guaranteed to be numerically stable and in which the error in time is quadratic. Alternatively, a smaller time step could have been used, albeit this would have made optimization extremely slow.

Errors in optimization

Errors in the optimization setup are difficult to quantify, but probably quite influencial here. The Levenberg-Marquardt algorithm is guaranteed to reach the local minimum within the set boundaries, and having set many different starting values with no effect on the results, it is quite evident that issues in the final results are not being caused by a failure of the algorithm to converge to the global minimum within the boundaries. Rather the most likely failure of the optimization procedure was overfitting. Namely, since the optimization was allowed to vary so many parameters, the individual parameters of interest were decoupled from the final results and only their relative values were fixed. This idea is expanded upon in Emissivity.

Emissivity

The intent of the experiment was to measure the emissivity of the rod in three different states: unaltered condition, covered with electrical tape, and buffed to be as shiny as possible. Our expectation was that these three states would each cause a distinct emissivity, with the taped rod having a higher emissivity and the buffed rod having a lower emissivity. This was not made evident by the data. Every run of our simulation optimization program resulted reaching the boundaries (either 0 or 1). The actual state of the rod had little to no effect on which of these two results were produced; the starting value we gave the optimization program tended to have more of an influence.

We believe that these aberrant results were due to either the design of the model or overfitting. In either case, the effect of the parameter had a negligible effect on the quality of the optimization, resulting in it consistently being fully maximized or minimized. In the eyes of the program the terms $\sigma(u(x,t)^4 - u_{\mathrm{amb}}^4)$ and $(u(x,t) - u_{\mathrm{amb}})$ are roughly of the same magnitude, and so it arbitrarily balances ϵ with k_c. Because the radiation term does tend to be bigger, it ends up maximizing ϵ and minimizing k_c. This unstable balanced is only halted by the manually imposed boundary on ϵ at 1 (the maximum physically possible). If we leave it unbounded, the program tends to increase ϵ and bring k_c to almost 0, because it is easier to optimize with just the one necessary term. Because we were unable to get any realistic values of emissivity, we decided that it would be better to state this fact than try to come up with an arbitrary uncertainty for a value that is obviously physically wrong.

Specific heat

Error Sources:

- Constant multiplication by mass density which was left variable

- Likely constant offset as density bounds did not include measured value

- The inverse has a linear relationship with the time derivative

Specific heat measurements yield a value with low relative error; however, error must still be accounted for, as there were multiple relevant sources. The primary source that may have affected the accuracy of our measurement is the fact that our measured mass density is lower than all of our simulation's calculated mass densities. (The minimum bound for mass density in the simulation was above the measured value). As these two values are always multiplied by one another for all terms in the temperature time-derivative model, this would lead to a lower value for the specific heat to account for the higher value for density. Furthermore, as the mass density was allowed to vary between simulation runs, unnecessary uncertainty was induced into the specific heat, as only their product mattered in the model. Another consideration for the specific heat's error is that its inverse is a linear factor of the heat exchange derivative and so any other linear effects over the rod, which would be accounted for in more complex models, could only be accounted for by varying the mass density and specific heat in the simulation.

Power fraction

Error sources:

- Heat loss from resistor is temperature dependent

- Rubber bands near power resistor

- Positive note, never exceeded actual value

One key issue is that the heat loss out of the power resistor into the environment, which is a portion that would not be transmitted to the rod and is dependent on the temperature of the power resistor for convection as well as radiation. The simulation model did not account for this, as it assumed that the power transmitted to the rod remained constant for the duration of the heating period. However, attempting to calculate this would have introduced the new variables of the power resistor's emissivity and convection coefficient which would have given the simulation further degrees of freedom and increased complexity of data verification and analysis. Another potential issue is the potential for power losses out through the rubber bands near the power resistor. As we had no thermocouples between the power resistor and the rubber bands any losses of power due to these could be seen as equivalent to power losses in transmission from the power resistor. On a positive note, however, the power fraction never went above 1 and so the simulation at the very least never over-estimated the power sent down the rod.

Convection coefficient

While properties of the rod and air, most of which are constant, must be used to calculate a convective coefficient, the temperature difference between the rod and air also contributes to the value of the convective coefficient. Thus, as voltage input and heating power varied the rate of change in temperature for the rod in different experimental trials, the convective coefficients found vary accordingly. Despite the fact that the values of convective coefficients follow a logarithmic curve such that the rate of change of these values decrease as the temperature difference between the air and the rod increases, it was impactful to the results of the experiment. The convective coefficients could also be affected by airflow in the lab (such as currents caused by people walking past the lab setup).

Thermal conductivity

While the variation in the conductivity parameter is very low due to the poor choice of optimization boundaries (the conductivity almost always hit the lower bound that we set), it is expected that the true measured value of conductivity would have varied by the influence of several physical factors. Holes made for temperature sensors disrupt the flow of heat along the rod and influence heat transfer. While rubber O-rings were selected for their low conductivity, their contact with the rod may have allowed for additional heat loss as well. Lastly, contact was made with the rod by experimenters on several occasions throughout the experiment to ensure proper heating, which also slightly contributes to uncertainty.

Chapter 6

Conclusion and Summary

The goal of this experiment was to determine the thermal conductivity, specific heat capacity, emissivity, and convective heat transfer coefficient of a rod, as well as the fraction of power generated by a power resistor that flowed down the rod, and to observe how these values change with the orientation and color of the rod. We obtained the following numerical results:

Thermal conductivity: 100.26 W/mK

Specific heat capacity: 370.55 ± 20 J/gK

Power fraction: 93.38% ± 10%

Emissivity: 0.9091 W/m^2 (not observed to change with different colored rod)

Convective heat transfer coefficient:

- Vertical: 8.40 W/m^{2}K
- Horizontal: 5.66 W/m^{2}K
- Diagonal: 6.63 W/m^{2}K

Overall, the obtained data was severely inconsistent and uncertain, and it is difficult to draw meaningful conclusions from our numerical results. Indeed, for many of the results, uncertainties could not even be assigned, as rigorously establishing bounds would be implausible.

It is suspected that this was due to a number of factors, most notably noise in the directly-measured temperature data and methodology used to estimate parameters from the temperature data. Possible improvements to the experimental procedure might include developing a better way to shield noise in temperature measurements, creating more sophisticated simulation and optimization techniques, and reducing the number of degrees of freedom the optimization has to account for by making more physical measurements.

Appendix A

Explicit Method of Finite differencing

The following is a description of the explicit method of finite differencing, demonstrated using the simple example of the one-dimensional heat conduction equation

$$\frac{\partial}{\partial t}u(x,t) = \alpha\frac{\partial^2}{\partial x^2}u(x,t). \tag{A.1}$$

Finite difference equation

In the explicit method for finite differencing, the temperature for each spatial point can be independently determined from the previous step. That is,

$$u_i^{n+1} = u_i^n + \alpha\cdot\frac{\delta t}{\delta x^2}\cdot\left(u_{i-1}^n - 2u_i^n + u_{i+1}^n\right), \tag{A.2}$$

where the superscript $n \in [0,T]$ signifies the step in time t_n and the subscript $i \in [0,X]$ represents the position x_i. δt and δx are the time steps in time and position respectively.

If we define

$$\zeta = \alpha\cdot\frac{\delta t}{\delta x^2},$$

then this can be written as a linear relationship

$$\mathbf{u}^{n+1} = \mathbf{D}\mathbf{u}^n, \tag{A.3}$$

where $\mathbf{D}$ is the matrix defined by

$$\mathbf{D}_{ij} = \begin{cases} \text{BC}, & i = 0 \text{ or } i = X \\ \zeta, & 0 < i < X \text{ and } |i - j| = 1 \\ 1 - 2\zeta, & 0 < i < X \text{ and } i - j = 0 \\ 0, & \text{else} \end{cases} \tag{A.4}$$

The top and bottom rows ($i = 0$ and $i = X$) are determined from boundary conditions. Note that as ζ approaches 0, $\mathbf{D}$ approaches the identity matrix. Thus ζ should be as small as possible for the best approximtation. The condition for stability is

$$0 < \zeta < 1. \tag{A.5}$$

Error in time

The explicit method uses a forward difference in time. The expression for the derivative approximation is derived from the power series expansion in δt

$$u(x,t+\delta t) = u(x,t) + \frac{\partial}{\partial t}u(x,t)\cdot\delta t + \frac{\partial^2}{\partial t^2}u(x,t)\cdot\frac{\delta t^2}{2!} + \ldots \tag{A.6}$$

Thus we have an approximation for the time derivative

$$\frac{u(x, t + \delta t) - u(x, t)}{\delta t} = \frac{\partial}{\partial t} u(x, t) + O(\delta t). \tag{A.7}$$

The error in time due to this approximation is linear in δt.

Error in position

The explicit method uses a central second derivative in space. The expression for the second derivative approximation is derived from the power series expansion in δx.

$$u(x + \delta x, t) = u(x, t) + \frac{\partial}{\partial x} u(x, t) \cdot \delta x + \frac{\partial^2}{\partial x^2} u(x, t) \cdot \frac{\delta x^2}{2!} + \frac{\partial^3}{\partial x^3} u(x, t) \cdot \frac{\delta x^3}{3!} + \dots \tag{A.8}$$

At $-\delta x$, this is

$$u(x - \delta x, t) = u(x, t) - \frac{\partial}{\partial x} u(x, t) \cdot \delta x + \frac{\partial^2}{\partial x^2} u(x, t) \cdot \frac{\delta x^2}{2!} - \frac{\partial^3}{\partial x^3} u(x, t) \cdot \frac{\delta x^3}{3!} + \dots$$

Thus the approximation for the second spatial derivative is

$$\frac{u(x - \delta x, t) - 2u(x, t) + u(x + \delta x, t)}{\delta x^2} = \frac{\partial^2}{\partial x^2} u(x, t) + O(\delta x^2). \tag{A.9}$$

The error in position due to this approximation is quadratic in δx.